Published: 6 June 2016

© Author(s) 2016. CC-BY 3.0 License.





Oxidation of sulphides and rapid weathering in recent landslides

Robert Emberson^{1,2}, Niels Hovius^{1,2}, Albert Galy³, Odin Marc^{1,2,}

¹GFZ Deutsches Geoforschungszentrum, 14473 Potsdam, Germany

²Institute of Earth and Environmental Science, University of Potsdam, 14476 Potsdam, Germany

³CRPG-CNRS-UL, 54500 Nancy, France

Correspondence to: robert.emberson@gfz-potsdam.de

Abstract

Linking together the processes of rapid physical erosion to the resultant chemical dissolution of rock is a crucial step in 10 building an overall deterministic understanding of weathering in mountain belts. Landslides, which are the most volumetrically important geomorphic process at these high rates of erosion, can generate extremely high rates of very localised weathering. To elucidate how this process works we have taken advantage of uniquely intense landsliding, resulting from Typhoon Morakot, in the Taimali river and surrounds in Southern Taiwan. Combining detailed analysis of seepage chemistry with estimates of catchment-by-catchment landslide volumes, we demonstrate that in this setting the primary role of landslides is to introduce fresh, highly labile mineral phases into the surface weathering environment. There, rapid weathering is driven by the oxidation of pyrite and the resultant sulphuric acid-driven dissolution of primarily carbonate rock. The total dissolved load correlates well with dissolved sulphate – the chief product of this style of weathering – in both landslides and streams draining the area ($R^2 = 0.841$ and 0.929 respectively, p < 0.001 in both cases), with solute chemistry in seepage from landslides and catchments affected by significant landsliding governed by the same weathering reactions. Bedrock landslides create conditions for weathering where all mineral phase in a lithology are initially unweathered within landslide deposits, and therefore the most labile phases dominate the weathering at the outset and during a transient period of depletion. This mode of dissolution can strongly alter the overall output of solutes from catchments and their contribution to global chemical cycles if landslide-derived material is retained in catchments for extended periods after mass wasting.

25

1. Introduction

Bedrock landslides can produce favourable conditions for weathering by funnelling of runoff into deposits of freshly broken rock mass with massive exposed mineral surface area and modest hydraulic conductivity. It has been shown in the Western Southern Alps (WSA) of New Zealand (Emberson et al. 2015) that this can give rise to strong gradients in dissolved solid concentrations in surface waters on hillslopes, with highest concentrations in seepage from landslides, and that the rate of landsliding is an important control on the chemistry of the rivers draining the mountain belt.

Localized landslide weathering, prone to the spatial and temporal variability of mass wasting, contrasts to common models in which weathering is controlled by steady and distributed erosion of a laterally continuous soil and regolith mantle (Dixon and von Blanckenburg 2012; Hilley et al. 2010). Such models anticipate that at high erosion rates weathering is kinetically limited, so that the link between material supply and weathering is progressively weakened and finally lost. Landsliding circumvents this by mobilizing relatively unweathered materials from deeper below the surface and, crucially, fragmenting them so that weathering is locally optimized. Landsliding is the dominant erosion process in orogenic settings where rapid crustal shortening is paired with fast and persistent exhumation (S. J. Dadson et al. 2004; Hovius, Stark, and Allen 1997). We expect, therefore, that it may act as a first order control on dissolved solids

Published: 6 June 2016

© Author(s) 2016. CC-BY 3.0 License.





export from active mountain belts. Here, we ask: does highly localised landslide weathering persist in different settings with variable lithology and climate, and can a more general case for the impact of landslides on weathering, including the underlying mechanism by which weathering is boosted, be made?

To address these questions, we have investigated chemical weathering in the rapidly eroding mountains of Taiwan at the local and catchment scale. Our study site has a substrate of typical continental margin sediments, comprising calcareous sandstones and shales, and containing sulphide minerals. This is a marked contrast with the WSA, where the metasedimentary silicate rocks contain only trace amounts of carbonate and very little pyrite. In this study, we exploit the synchronous occurrence of voluminous mass wasting in southern Taiwan due to exceptional rainfall associated with typhoon Morakot in 2009 to eliminate the effects of progressive loss of soluble minerals, allowing a sharp focus on the causes of elevated weathering rates in recent landslides. Using samples of seepage from recent bedrock landslide deposits and water from mountain streams and rivers paired with catchment-wide estimates of landslide volume, we show that enhanced weathering in landslide deposits results primarily from the rapid reaction of the most labile minerals in the substrate, which are excavated from below the saprolite-bedrock interface by deep-seated slope failure. In the case of our Taiwanese site, the oxidative weathering of highly reactive pyrite and the ensuing rapid sulphuric acid-driven weathering of carbonate dominate the output from recent landslides and propagate importantly into the stream chemistry.

2. Field Sites and sampling

60 The mountains of Taiwan have erosion rates that are amongst the highest on Earth (between 4-6mm/yr (Willett et al. 2003; Fuller et al. 2003)), driven by rapid tectonic convergence at the East Asian margin and aided by tropical storm activity and earthquakes (S. Dadson et al. 2003). Average annual mass-wasting rates are high (Hovius et al. 2000), but can be pushed to much higher rates by single, exceptional storms or seismic activity (Hovius et al. 2011; G.-W. Lin et al. 2008; Marc et al. 2015). For example, in 2009 typhoon Morakot caused over 2.7m of rain in 48 hours (Chien and Kuo 2011) on the Southern part of the island, the highest storm totals ever recorded in Taiwan. The typhoon generated more than 22000 landslides (C. W. Lin et al. 2011; A J West et al. 2011), with an average density of 35000 m²/km², orders of magnitude more than under less exceptional meteorological conditions. This presents a rare opportunity to study an extensive population of recent, synchronous landslides, which is important because the rapid weathering in landslides might decay over a decadal time scale to levels indistinguishable from that on surrounding hillslopes 70 (Emberson et al. 2015). Having a constant, known date of initiation for sampled landslides reduces any systematic changes to weathering that would be introduced by variable timing of the mass wasting. Moreover, having a total landslide surface area and volume dominated strongly by input from one single typhoon makes the solute load of rivers draining catchments with otherwise diverse landslide histories directly comparable. We sampled water chemistry from a variety of sources within the Taimali river catchment (Fig. 1b) between February 75 and March 2015. This catchment drains an area of 118km² in the East flank of the Taiwan Central Range, from the main divide to the Pacific Ocean. It had among the highest catchment landslide densities resulting from typhoon Morakot, with several subcatchments catastrophically alluviated by debris. As a result, human settlement and activity in the catchment were abandoned inward of 7km from the coast, and at the time of sampling, anthropogenic influence was negligible. In addition to the Taimali main stream, we sampled seepage from the deposits of 14 landslides, representing water draining through the landslides, either directly from rainfall or from runoff into the crests of landslides, stream water from 19 subcatchments with areas between 1-10km², and geothermal spring water. We supplemented our

Published: 6 June 2016

95

110

115

120

© Author(s) 2016. CC-BY 3.0 License.





landslide seepage samples from the Taimali catchment with seepage from 8 recent landslides elsewhere in Southern Taiwan (Fig.1A), to assess landslide weathering over a wider range of locations.

Lithologically, the Taimali catchment is representative of the Tertiary sedimentary cover that forms a large proportion of the Taiwanese orogen (Central Geological Survey 2000); the slates, shales and sandstones of the Miocene Lushan and Eocene Pilushan formations contain important amounts of sedimentary and diagenetic carbonate and are pyrite bearing throughout (Das, Chung, and You 2012). The sampled landslides outside the Taimali catchment are also rooted in the Pilushan formation, with the exception of two landslides in the Chenyoulan catchment in central West Taiwan, underlain by the Eo-Oligocene Paileng formation of slates and sandstones. The lithologies of the sampled formations are the dominant sedimentary rocks formed at continental margins with a clastic input, and they are found globally in active mountain belts.

Sampled landslides vary in size between 7.6x10³-2.8x10⁶m², and their deposits cover a range of shapes. The largest landslides in the Taimali catchment initially blocked the main river channel and have since been incised, leaving massive fan terraces, tens of metres above the current river level. Intermediate landslides have built debris cones on hillslopes and at the edges of valley floors, and some smaller landslides have filled debris chutes. All sampled landslides had mobilized bedrock in addition to the overlying regolith and soil mass and any present vegetation. In the Taimali catchment and at other landslide sample sites, the modal topographic slope is around 26°, with many steeper hillslope segments. This precludes the build up of a thick, laterally continuous soil and regolith mantle, and bedrock is present at or near the surface except where local colluvial fills have formed.

Seepage was found at the base of many landslide deposits, immediately above the interface with underlying bedrock. The flow paths of this seepage could enable fluid interaction with exposed rock in the landslide scar as well as fragmented rock mass in the deposit. We do not draw distinction between these, as the physical process of bedrock landsliding remains responsible for the exposure of the scar and the production of the deposit. Moreover, it is not possible to distinguish systematically between landslide scar and deposit from available satellite imagery. Landslide seepage may also incorporate deeper groundwater, which could exfiltrate through the scar. In view of this, we correct our samples for any geothermal input.

Notably, during the early part of 2015, when we sampled, the South of Taiwan underwent one of the driest periods on record, with an estimated return time of 50-100 years (CWB (Central Weather Bureau) 2016). At this time, the sampled streams were at or close to a baseflow condition, but despite the dry conditions more than half of the deep-seated landslides we visited had persistent seepage. Therefore, it seems probable that many landslides in Southern Taiwan are never fully 'dry' in the current climate. Landslides in the Chenyoulan catchment were sampled in July and November of 2013, when more normal rainfall conditions prevailed.

Further, it is important to note that the sediment generated by landslides and debris flows does not reside exclusively on the hillslopes from where it was sourced. Significant storage of material over long timespans in larger river channels is common, and is indeed substantial along the Taimali River, with channel fill occupying about 6% of the total catchment area. This channel fill may be an important weathering reservoir, and to investigate whether this stored sediment affects the observed river chemistry we have mapped the fill deposits along sampled streams.

Since we sampled small seepages and 1st order tributaries, we lack good constraints on the fluxes of solutes. Discharge gauging is not available in the Taimali, as the hydrometric infrastructure on the river was destroyed by channel bed aggradation after typhoon Morakot. Here, we report measured solute concentrations in landslide seepage and stream waters with unknown flow rates. These measurements can't be converted into solute fluxes without major assumptions,

© Author(s) 2016. CC-BY 3.0 License.





and weathering flux estimation is not the purpose of this study. Instead, we aim for a direct comparison of landslide seepage and river chemistry from a set of lithologically similar streams with identically timed mass wasting but varying populations of landslides.

125

130

135

3. Analytical techniques

Samples were collected from source using an HDPE syringe, filtered on site through single-use 0.2µm PES filters into several HDPE bottles, thoroughly rinsed with filtered sample water. Samples for cation analysis were acidified using ultrapure HNO₃·. pH and temperature values were measured in the field at the time of sample collection.

Analysis of cations was carried out with a Varian 720 ICP-OES, using SLRS-5 & USGS M212 as external standards, and GFZ-RW1 as an internal standard and quality control (QC). QC samples were included for every 10 samples to account for drift; no systematic drift was found, with random variability less than 5%. Sample uncertainties were determined from calibration uncertainties, and were always lower than 10% (see Table 1 for element-specific uncertainties). Anion analysis was performed using a Dionex ICS-1100 Ion Chromatograph, using USGS standards M206 & M212 as external standard and QC. Uncertainties were always less than 10% for each of the major anions (Cl⁻SO₄²⁻, and limited NO₃·). Bicarbonate (HCO₃·) was calculated by charge balance, and the calcite saturation index of

3.1. Correction for cyclic input

Solute input from atmospheric sources is small but significant in the Taimali and at most other locations where we have sampled landslide seepage. Several studies have measured the average rainfall chemistry in different parts of Taiwan, finding that it is highly dependent on both location (e.g. higher pollutant content near the densely populated west coast (Wai et al. 2008) and intensity of rainfall (typhoon rainfall boasts the highest solute concentrations in some cases (Cheng and You 2010)). However, we found that using any of these published values for correction resulted in clearly erroneous estimates of the proportion of cyclic salts in the water samples (e.g., >100% of dissolved K⁺ and SO₄²⁻ from cyclic sources). Therefore, we have applied a correction to all samples based on ratios of dissolved species in seawater. The Taimali catchment lies within 15km of the ocean, within the first orographic barrier, which supports the use of seawater ratios. Other sample sites are more widely spread but we prefer a single correction to a piecemeal, individual treatment. Using the ratios of Cl⁻ to major cations and anions (Ca²⁺, K⁺, Mg²⁺ and Na⁺, and SO₄²⁻) in seawater and assuming that all Cl⁻ present in samples results from cyclic contribution, we removed extrapolated cyclic cation and anion contributions according to the following equation:

measured waters was determined using the USGS PHREEQC software package (Pankhurst and Appelo 2013).

$$[X]_{\text{cyclic}} = [Cl^{-}]_{\text{sample}} \times ([X]_{\text{rainfall}}/[Cl^{-}]_{\text{rainfall}}) (1)$$

Where [X] is the measured concentration of any of the dissolved species. The assumption that all Cl⁻ results from cyclic input is conservative and justified as there are no evaporitic units reported in the sampled areas (Central Geological Survey 2000; Ho 1975), and because the Taimali catchment and most of the other landslide sites are essentially free from anthropogenic chemical input. Chloride is a minor component in all samples, with a median value of 32 μmol/l (minimum 14.6, maximum 175 μmol/l). This is a similar range of values to rainwater measured in other coastal
environments (Galloway et al. 1982; Nichol, Harvey, and Boyd 1997). Individual corrections for cyclic input are small; only Sodium has larger corrections as in some cases approximately 20% of the total molar concentration is derived from

Published: 6 June 2016

© Author(s) 2016. CC-BY 3.0 License.





cyclic sources, and the average correction is 10%.

3.2. Mapping of landslides

165 We mapped landslides extant in the Taimali and surrounds prior to typhoon Morakot and those generated during and after the event until 2015 from LandSat imagery (LS7 & LS8, resolution 30 and 15m respectively). Landslides generated during typhoon Morakot were also mapped from a mosaic of Formosat images taken within one month of the typhoon with a resolution of 2m. Landslides were identified manually, based on their geometry, topographic position and surface properties, as prescribed by recent studies (Marc and Hovius 2015), and digitized on screen in an Arc-GIS 170 environment; scars and deposits were mapped together as a clear distinction was not always possible from the available imagery. Manual mapping prevents the inclusion of other active landscape elements with recent reflectivity changes, for example aggraded riverbeds, which were mapped separately. It also suppresses the possibility of amalgamation of multiple landslides into single mapped polygons, which blights automatic mapping (Marc and Hovius 2015). In our analysis we draw distinction between older landslides and those generated by typhoon Morakot, especially in the 175 context of previous work (Emberson et al. 2015) that has shown the chemical output from individual slides is likely to significantly decay over a decadal timescale. It should be noted that the proportion of landslides predating typhoon Morakot is dwarfed by the mass wasting caused by this exceptional typhoon in much of the Taimali catchment. The proportion of the Taimali catchment occupied by landslides increased from 2% to 8% due to typhoon Morakot, while some subcatchments have upwards of 16% of their area occupied by typhoon-induced landslides. However, in a few 180 subcatchments there is a larger proportion of older landslides, which allows for comparison with landscape units with only negligible prior mass-wasting.

4. Measured water chemistry

185

Concentrations of Total Dissolved Solids and major cations and anions in landslide seepage and stream water in the Taimali catchment and elsewhere in Taiwan are listed in Table 1.

TDS in seepage from sampled landslides in Taiwan ranges between 7200 μ mol/l to 23400 μ mol/l, while river TDS values lie between 4000 μ mol/l and 12600 μ mol/l. Thus, the measured total dissolved solids (TDS) in seepage from sampled landslides is consistently higher than in other surface water sources, with the exception of geothermal springs (up to c.100150 μ mol/l)

Dissolved Calcium is the major cation in most samples, forming up to 90% (molar) of the cation load in some cases. In some seepage samples this is replaced by Magnesium, with Mg²⁺ as much as 70% of total cations. Sodium and Silicon make up much of the remainder of the cationic load, although Silicon never represents more than 10% molar, while Sodium only exceeds 15% in three seepage samples. All measured samples are supersaturated with respect to calcite (Table 1). The anion load is always more than 50% Bicarbonate; the remainder is formed of Sulphate, SO₄²⁻, which is always more than 10% and can be as much as 50%. Seepage from the two sampled landslides in the Chenyoulan catchment share the same overall relationships between individual elements as those sampled in the Taimali catchment, and they both sit at the higher end of the range of concentrations. There is significant overlap between landslides sampled within the Taimali river and those in the immediate surrounds (Fig.1A); TWS15-68 is the most notable, with relatively elevated SO₄²⁻ and TDS (4078 and 14932 μmol/l respectively).

The concentrations of TDS in the streams of the Taimali catchment are systematically lower than in landslide seepage, but high in a global riverine perspective, 4141-12200 μmol/l. Ca²⁺ is again the most significant cation, always forming

© Author(s) 2016. CC-BY 3.0 License.





more than 21% and as much as 37% of TDS; Na^+ , Si^{4+} , and K^+ are minor components, always less than 7%, 6% and 1% of TDS, respectively. Mg^{2+} is quite variable; in most streams it only forms 1-3%, but it constitutes as much as 11% of the cationic load in three of the streams. In the anion load, HCO_3^- is often the most important component, forming between 20-50% of TDS. Sulphate is between 5 and 31% of TDS and exceeds HCO_3^- in six streams. We also measured trace strontium, with peaks at 30 μ mol/l. Lithium in the streams and main river is always below the detection limit of the OES (c.0.1 μ mol/l).

5. Discussion

210

205

5.1. Landslide weathering

Seepage from landslides in the Taimali catchment and scattered locations elsewhere in Taiwan has high TDS concentrations when compared with local streams. This supports the hypothesis that landslides are primary seats of rapid weathering in this setting. We have found the same in the WSA of New Zealand (Emberson et al. 2015), and 215 therefore the intense fragmentation of newly exposed rock mass and the concentration and slow percolation of rain and runoff water in debris accumulated in topographic hollows are likely universal mechanisms promoting landslide weathering in steep mountain settings where distributed weathering in soils is less efficient. In the WSA, TDS concentrations in landslide seepage are strongly impacted by the dissolution of trace calcite which is likely to be more abundant at depth (Brantley et al. 2013). The depth of a landslide scales with the area (Larsen, 220 Montgomery, and Korup 2010), implying that the proportion of calcite available correlate with the size of the issuing landslide. Where substrate mineralogy is relatively uniform, this size effect may be due to the greater depth of the scars and deposits of larger landslides, the mobilization of relatively less weathered rock mass and its more comprehensive fragmentation, and the reduced hydraulic conductivity at the base of such landslides. However, these effects are not evident in the Taimali catchment; R2 values for TDS / landslide area and TDS / landslide volume are -0.025 and -0.009 225 respectively (p = 0.706, p = 0.772, respectively). This suggests that here, other factors have an overwhelming effect on landslide weathering efficiency. Notably, we find strong correlations between the TDS and Ca²⁺ and dissolved Sulphate concentrations in landslide seepage ($R^2 = 0.841$ and 0.891, respectively; Kendall's Tau value of 0.5238 and 0.6381, respectively; p <0.001 in both cases; Fig 2a and 2b). We attribute this to the oxidation of pyrite in the mobilized and fragmented rock mass and an ensuing increase in weathering of carbonates driven by sulphuric acid. Although the 230 sporadic presence of other sulphide minerals, or mineral sulphates, can't be excluded, this has not been documented in Southern Taiwan. Instead, the rapid oxidation of pyrite has previously been observed in the region and elevated TDS concentrations in Taiwan mountain rivers have been viewed in this light (Calmels et al. 2011; Das, Chung, and You 2012; Kao et al. 2004). Sulphide oxidation is so prevalent in the larger Kaoping basin (draining the South Western part of Taiwan) that the delivered sulphate is 1.2-1.6% of global fluxes, from a basin only ~0.003% of global drainage (Das, 235 Chung, and You 2012), and these prior studies link this explicitly to elevated physical disintegration of rock. The lack of correlation between landslide size and seepage concentration suggests that the distribution of pyrite is highly heterogeneous, or that the degree of its exposure for oxidation varies significantly between different sites. The importance of pyrite in landslide weathering in Taiwan is disproportionate with its relatively minor abundance in the overall rockmass (Das, Chung, and You 2012; Kao et al. 2004). Instead, its prominent role is determined by its 240 reactivity. By introducing significant quantities of fresh rock material into the surface weathering zone, landslides reset the proportions of individual minerals within this zone to that of the deeper substrate. This removes the supply limit on

Published: 6 June 2016

245

250

255

260

© Author(s) 2016. CC-BY 3.0 License.





weathering for any phase, and allows rapid weathering of the most labile minerals present. In the Taimali and surrounds, the oxidation of pyrite is an important reaction in recent landslide deposits. It provides a potent source of acidity, which further accelerates the weathering of other minerals. The majority of the high TDS in landslide seepage is accomplished through carbonate weathering via either this sulphuric acid or carbonic acid. Calcium can also be sourced as a product of silicate weathering. However, the lower proportion of purely silicate derived cations in landslide seepage (e.g. Si:Ca²⁺ ratio), as well as the markedly different behaviour of some silicate derived cations, with the exception of broadly increasing K⁺ concentrations from c.20-300µmol/l over the measured range of SO₄²⁻, supports the interpretation that weathering in the sampled landslides is dominated by the dissolution of carbonates.

An implication of our observations is that in the Taimali catchment, a significant proportion of the sedimentary pyrite contained within the rock mass survives exhumation, and is only exposed by landslide fragmentation at the surface. Previous studies in Taiwan (Calmels et al. 2011) have shown that Sulphate is importantly present in deep circulating groundwater, but it is unlikely that such water would systematically surface at landslide sites, since individual landslides have highly variable morphologic characteristics (size, scar/deposit ratio, proximity to major faults). The same argument applies to geothermal outflow. Moreover, hot spring waters sampled in the Taimali catchment have extremely high Lithium concentrations, 1610 µmol/l, and the lack of elevated Li⁺ concentrations in the landslide seepage samples precludes a deep geothermal source for this outflow. Other studies have found high concentrations of silicate derived cations in deeper groundwater (Calmels et al. 2011); we do not observe any strong link between the concentrations of cations exclusively sourced from silicate minerals (Sodium, Silicon) and Sulphate in landslide seepage; extremely elevated Na⁺ and Mg²⁺ concentrations at some sites are not clearly associated with any other measured parameter, or with each other, and we have no ready explanation for these isolated observations at present.

5.2. Landslide weathering products in stream water

To directly compare the impact of landsliding on weathering in the steep mountains of Taiwan between landscape units 265 with variable landslide activity, we have used the volumes of landslides calculated for each sampled subcatchment within the Taimali drainage area, normalised to catchment area and evaluated this against the solute load of the streams. For this purpose, we use landslide volume rather than surface area, because much of the weatherable mineral surface area is contained within the landslide debris, rather than at the landslide surface. In doing so, we assume that the hydraulic connectivity in the groundmass of the landslide is always high enough to wet the mineral surface area within 270 the entire landslide body. We find that TDS and Ca²⁺ increase with increased landslide volumes in the sampled subcatchments where the landslide volume density tops approximately 10⁴m³/km² of catchment area (Fig. 3). Above this 'threshold', we observe a doubling of TDS from c.6000 to more than 12000 µmol/l and increases in the concentration of Ca²⁺ from c.1000 to nearly 5000 µmol/l, as landslide densities increase up to c.10⁶ m³/km². There is an increase in the SO₄² over this same landslide density range, from c.300 to nearly 4000µmol/l, and as in the individual landslide 275 seepage samples, there is a strong correlation of both stream TDS and dissolved Ca2+ concentrations with the dissolved Sulphate ($R^2 = 0.929$ and 0.9318, respectively; p<0.001 for both relationships). Dissolved SiO₂ (Fig.4b) and Na⁺ do not systematically vary with SO_4^{2-} (p = 0.92, p = 0.56 respectively), although K⁺ does increase significantly, from 15-130μmol/l with Sulphate concentration (p <0.001). At lower specific landslide volumes, there is a larger degree of variability and below 104m3/km2, equivalent to a debris layer with a uniform thickness of about 1 cm over the 280 catchment, the stream TDS and Ca²⁺ concentrations do not vary systematically with the landslide volume. The importance of landsliding in setting the chemical load of streams varies depending on which element is considered.

Published: 6 June 2016

320

© Author(s) 2016. CC-BY 3.0 License.





For example, landslides exert a strong control over dissolved Calcium and Potassium in streams, but have almost no impact on dissolved Sodium. At the catchment scale, solute concentrations remain primarily dependent on the additional acidity provided by oxidation of pyrite; coupled carbonate-sulphuric acid weathering increases the Ca2+ output, and with 285 it of the total exported solute load. On the other hand, dissolved SiO2 is unaffected by either increasing landslide volume or changes in SO_4^{2-} . Notably, values of SiO_2 measured in the streams of the Taimali catchment can exceed those measured in landslide seepage, suggesting that any landslide-induced impact on local silicate weathering is not significant enough to outweigh weathering elsewhere, either in soils on stable hillslopes or deeper in the subsurface. Longer flow paths of deep groundwater, reaching well below the levels affected by landsliding, are more likely to be 290 enriched in slower dissolving silicate weathering products (Bickle et al. 2015; Calmels et al. 2011; Galy and France-Lanord 1999), and the relatively low fraction of Silicon in landslide seepage suggests a comparatively short water residence time in mass wasting deposits (Maher 2011). In view of this, we posit that the disconnection between streamborne Sulphate and some silicate-weathering products (Na⁺, SiO₂), juxtaposed with a link of Sulphate and Potassium, which is also only sourced from silicate, reflects the existence of multiple pathways relevant for silicate weathering on a 295 catchment scale. More congruent weathering in deep groundwater likely complements the rapid weathering of carbonates and incongruent weathering of silicates (such as rapid K release by chlorite and biotite, (Malmstrom et al. 1996)) in mass wasting deposits. The sampled subcatchments have up to 16.6% of the total area occupied by landslide deposits and scars. However, the Taimali watershed contains some exceptionally large landslides, the outlines of which define tributary catchments in 300 their own right. The largest landslide we sampled (TWS15-46) has a surface area of 2.7km². At these very large scales and where landsliding has affected such an important part of the topography, saturation of the surface water chemical load is likely. This depends on the local distribution and exposure of sulphides and, since rainfall is dependent on area, also on the area:volume ratio of the landslides, which limits the amount of fluid for dissolution per unit landslide volume. Therefore, it is likely that the relationship between landslide volume and stream solute concentration will also 305 saturate above a hypothetical "maximum concentration" in seepage from landslides above a given size. In the landslides sampled in and around the Taimali river, this maximum TDS appears to be around 15000-20000µmol/l, which we observe in landslides 50000m² and larger (although larger slides can remain below this point). Even where landsliding is less prominent, there is still significant variability in tributary stream dissolved load (Fig.3). This is unlikely to be an artefact of the mapping; landslides below the detection limit (about 500 m²) are unlikely to 310 mine significant quantities of bedrock. Instead, they primarily mobilize colluvial or soil material, which limits their impact via the oxidation of sulphides. Meanwhile, other environmental factors that result in variability in TDS at higher landslide rates will also apply to the steep mountain landscape of southern Taiwan in the absence of landslides. This includes variable oxidation of pyrite in a tectonically fractured substrate, which will affect both deep and shallow groundwater fluxes, depending on where in the weathering zone the respective hydrological flow paths locate. Other studies have incorporated topographic factors into the models of weathering (Heimsath et al. 1997; Maher and 315 Chamberlain 2014), and these may also be a source of variability at low landslide rates. Since the intensity and volume of rainfall during the typhoon were the primary control on the rate of landsliding during typhoon Morakot (C. W. Lin et al. 2011), the pattern of landsliding in the Taimali catchment is not strongly tied to topographic characteristics. Hence, the amount of mass-wasting in individual sub-catchments is not strongly related to the local modal slope.

importantly from landslide debris delivered to streams. Alluviated streambeds could be a locus of enhanced weathering,

Many subcatchments of the Taimali watershed contain significant amounts of alluvial material, which derives

Published: 6 June 2016

330

335

340

345

350

355

360

© Author(s) 2016. CC-BY 3.0 License.





but we do not observe any correlation between the measured stream chemistry and the proportion of the catchment filled with alluvial material in the six subcatchments with significant fill (>1% of total catchment area – see Table 1. R^2 = -0.365; Kendall's Tau = -0.067; p = 0.48). However, due to the lack of rainfall prior to and during the sampling 325 period we were unable to sample hyporheic water from within the alluvial streambeds. Presence of secondary precipitates in fill deposits suggests that at low flow these sedimentary bodies could act as sinks for solutes, rather than sources. Although the role of alluvial materials in the weathering budget of the Taimali catchment is not fully clear, our observations suggest that it is not a first order control on the chemical output during the sampling interval. Since we did not measure the discharge in these small streams we can only report concentrations of solutes. Weatherdetermined dilution could affect the measured solute concentrations and cause it to vary between catchments. However, observations from other parts of the Taiwanese mountains (Calmels et al. 2011) suggest that dissolved Calcium and SiO₂ concentrations do not dilute by more than approximately 35% for the full range of discharge conditions in mountain rivers. Therefore, we expect that although the period when we sampled was relatively dry, our measurements are a fair first order representation of solute concentrations and ratios during the majority of the year. This is in keeping with observations from other mountain belts, including the Southern Alps of New Zeanland and the Himalayas, where rivers are quite close to chemostatic over a range of discharge conditions (Lyons 2005; West, Galy, and Bickle 2005).

5.3. Landsliding and the weathering of labile minerals

Solute concentrations in landslide seepage and stream water in the Taimali catchment are significantly higher than in the rivers of the WSA by approximately 5-10 times (Fig.3a). Both locations share a steep, landslide-dominated mountain physiognomy and very high rainfall rates, but Taiwan is warmer and has carbonate rich, pyrite bearing lithologies, whereas the WSA formations have only trace amounts of these minerals. We suggest that lithology and climate set a baseline for weathering in a given setting, above which landslides can control the weathering variability. This control is especially clearly expressed in the WSA, where the substrate for weathering is relatively homogeneous. The Taiwanese river chemistry has a larger spread with respect to landslide volumes, but the clear correlation between stream TDS and SO₄² (Fig.4) reflects the importance of the weathering occurring within the landslides in setting catchment scale river chemistry. Heterogeneous distribution of sulphides in the bedrock substrate of the Taimali catchment and its variable oxidation during exhumation not only affect the individual landslide seepage concentrations, but also the chemistry of streams throughout the catchment. This may explain why the total volume of landslides is a weaker control than in New Zealand.

Reactions of the most labile mineral phases dominate the chemistry of landslide seepages. In the Taimali catchment and elsewhere in Taiwan, the fastest reaction is the oxidation of sulphide. In the case of the WSA, elevated landslide seepage concentrations (Emberson et al. 2015) result from weathering of small amounts of highly labile carbonate, which become exposed through rock mass fragmentation. However, unlike the Taimali, the fragmentation of WSA bedrock does not introduce an extra source of acidity. The relative abundance of carbonate in Taiwan means fluids are supersaturated everywhere with respect to Calcium (Table 1). Therefore, the potential for landsliding to increase carbonate weathering due to rock mass fragmentation would be limited but for the exposure of pyrite and the generation of sulphuric acid this entails. Thus, exposure of minority minerals due to rock mass fragmentation boosts weathering rates in landslides, but the minerals and their roles vary between settings. We describe this style of weathering as nonequilibrium weathering, as the depletion rates of the various minerals involved are likely to be very different. Landslide weathering rates will remain elevated until the relevant minority mineral(s) have been depleted, after which

Published: 6 June 2016

© Author(s) 2016. CC-BY 3.0 License.





weathering in landslides is likely to proceed much like in other parts of the landscape. The initial abundance of trace sulphide and/or carbonate together with their exhaustion, over longer time scales, is likely to be an important control on the duration of rapid weathering in landslides. However, in choosing the Taimali catchment, where the vast majority of 365 the mass wasting observed occurred very recently and all at once, we have also selected a location where the long-term impact of rock mass fragmentation in landslides is difficult to observe. Nevertheless, some constraints may be gleaned from two subcatchments (TWS15-40 and TWS15-53) where the TDS and dissolved SO₄²⁻ values are lower than others with similarly high landslide incidence (TWS15-40 9220µmol/l, TWS15-53 7617µmol/l compared to other streams with TDS greater than 12000µmol/l). These two subcatchments have large landslides that had been moving persistently for at 370 least two decades prior to typhoon Morakot. Although these landslides were reactivated during the typhoon, they likely displaced materials that had already been significantly depleted of pyrite due to prior fragmentation and weathering. This is circumstantial evidence of a substantial loss of weathering efficiency by depletion of especially labile minority minerals on a decadal time scale in this instance, similar to previous findings in the WSA (Emberson et al. 2015). A second time scale of relevance is that of the physical removal of landslide debris from the catchment. If debris 375 remains in a catchment after depletion of exposed pyrite, then its weathering will revert to mineral reactions with Carbonic Acid, which dominate elsewhere in the landscape. If the time to depletion is greater than the time required for removal of the debris, then the labile phases it contains will remain unweathered and will be removed through sediment transport processes. In the case of Taiwan, restricted data on river bed material show Sulphur content of up to 1.07% (Hilton et al. 2014), suggesting that weathering in the landscape does not purge all sulphides brought to the surface by 380 rock mass exhumation. In the opposite case the weathering from a given landslide will return to a constant background rate shared with other, colluvium and soil covered parts of the landscape. How this scales up to the catchment scale depends on the return time of large drivers of mass-wasting, such as typhoons and earthquakes, and the subsequent advection of debris into the fluvial network and the transport capacity of this network. A disparity between short term production of sediment on hillslopes and the capacity for onward transport can lead to up to millenial residence times of 385 event-produced sediment in mountain landscapes (Blöthe and Korup 2013). In the Taimali catchment, many headwater streams were still clogged with sediment 6 years after typhoon Morakot, and large colluvial fans had formed below several landslide-dominated tributaries. Elsewhere in Taiwan, mountain valleys contain large colluvial terraces, which have formed hundreds to thousands of years ago (Hsieh and Chyi 2010). This implies that time scales of pyrite depletion and of debris removal must both be considered in further explorations of the links between erosion and 390 weathering in Taiwan.

5.4. Impact on climate

395

400

The link between weathering and atmospheric pCO₂ is determined by the mineralogy of the weathered substrate, the composition of the weathering acid, and the residence time of material in the weathering zone. Therefore, the balance of silicate:carbonate weathering, the source of acidity in mass-wasting deposits and the retention of these sediments in the landscape are all crucial to the role of landsliding in the Carbon cycle. As a result of this complexity, the impact of landsliding on climate is ambivalent. Weathering of silicates with Carbonic acid can lower the atmospheric pCO₂, but with Sulphuric acid it has no effect. Dissolution of carbonates has no net effect on atmospheric pCO₂, if achieved with Carbonic acid, and it can increase pCO₂ if it is accomplished with Sulphuric acid (Calmels et al. 2007; Gaillardet et al. 1999; Torres, West, and Li 2014). As erosion rates increase and mass-wasting through bedrock landsliding begins to dominate erosional budgets, the feedback between drawdown of CO₂ and erosion, achieved through sustained

Published: 6 June 2016

© Author(s) 2016. CC-BY 3.0 License.





weathering of silicates (Berner and Kothavala 2001; Brady 1991), will weaken. Then, weathering of carbonates will assume a more central role, even where they are only present in small amounts, and in mountain belts where pyrite is ubiquitous, erosion-driven weathering may even become a source of CO₂. If the retention time of sediment derived from mass-wasting is long compared to the decay time of the weathering boost provided by these highly labile minerals, then any effect of landsliding on the CO₂ budget of a mountain belt may be limited. As the sediment retention time equals the weathering boost decay time, the effect of landsliding on the CO₂ budget is maximized. Shorter sediment residence times promote the export of unweathered sediment to the ocean and its burial in marine basins. This can result in a fraction of sulphides contained in the rock mass bypassing the weathering window (Hilton et al. 2014), reducing the potential effect of their exhumation on atmospheric pCO₂ and returning the landscape to a state in which distributed weathering in soils and colluvial fills dominates. In addition to this inorganic complexity, the export and burial of organic carbon via landsliding also has an impact on the Carbon budget of a mountain belt (Hilton, Galy, and Hovius 2008; Hilton et al. 2011; West et al. 2011). Ultimately, quantification of the processes side by side is important to understanding of the role of mountain erosion in the Earth's Carbon cycle.

In the Taimali catchment – a good analogue for many young mountain belts formed of continental margin sediments – widespread, typhoon-triggered landsliding has caused a significant increase in carbonate weathering by Sulphuric acid over timescales shorter than the return time of extreme meteorological drivers of mass wasting. As a result, the area most affected by erosion due typhoon Morakot is now a net source of CO₂ to the atmosphere, unless the offshore burial of organic carbon eroded from soils and standing biomass in the landscape offsets this effect. The weathering boost is likely to end before the next major meteorological perturbation of southern Taiwan, so that the weathering of carbonates and silicates with Carbonic acid must be taken into account when considering the longer-term effects of erosion in South Taiwan.

6. Conclusions

425 Landslides can mobilize and fragment large volumes of rock mass from below the soil and regolith mantle of steep hillslopes. Weathering of this material is promoted by the exposure of fresh rock to persistently circulating water and oxygen in landslide debris with very high internal surface area. Under these conditions, weathering is not limited by the supply of weatherable material. It progresses, instead, at a rate determined primarily by the kinetics of the dominant chemical reactions, for as long as all minerals involved in these reactions are abundantly exposed. Thus, the process of 430 weathering in landslides is dominated in the first instance by reaction of the most labile mineral phases in the mobilized rock mass. We have found that these may be minority constituents, driving the weathering in fresh landslide deposits away from the slower process affecting the surface materials elsewhere in the landscape over longer time scales. In Southern Taiwan, weathering in landslides triggered during typhoon Morakot in 2009, is governed by the rapid oxidation of pyrite, which is a trace mineral in the pelitic units of the local substrate. This generates sulphuric acid, 435 which reacts primarily with ubiquitous carbonates. Five years after landsliding, carbonic acid is a weathering agent of lesser importance and the weathering of silicate minerals is subsumed. In the Taimali catchment in Southeast Taiwan, which sustained landsliding at spatially diverse rates during typhoon Morakot, stream chemistry suggests that landslides have tapped into rock mass with variable amounts of pyrite. Although total dissolved solids concentrations in tributary streams vary with the landslide density in their subcatchments, they are related first with the Sulphate concentration. In 440 rare subcatchments where older landslides, dating back at least 25 years, dominate, TDS and Sulphate concentrations are markedly lower, indicating that the effects of exposure and oxidation of pyrite in landslides may dissipate on

Published: 6 June 2016

445

450

455

460

465

480

© Author(s) 2016. CC-BY 3.0 License.





decadal time scales in this area.

Southern Taiwan sits within a rapidly deforming and uplifting mountain belt, formed with calcareous sandstones and pelites from the Asian continental margin. It shares its deformation style and a range of lithologies with many other young mountain belts at convergent plate boundaries. Bedrock landsliding is the dominant mode of mass wasting and sediment production in such settings. Therefore, we submit that our observations of landslide weathering in Taiwan may well have wider implications. Moreover, even where pyrite is not significantly present, the importance of labile mineral phases in weathering in recent landslide deposits is evident. In the Western Southern Alps of New Zealand, the rapid reaction of carbonates, which make up only a very small fraction of the rock mass, with carbonic acid dominates the chemistry of landslide seepage and helps set the weathering flux from the mountain belt.

Hence, in order to understand chemical weathering rates from mountain belts where erosion is dominated by stochastic mass-wasting it is crucial to consider the way in which this specific erosive process controls weathering. We propose a conceptual model of a rapidly eroding landscape where the background weathering is set by lithology and climate, overprinted by the impact of landslides. The importance of minor lithological phases, weathering rapidly in small and specific parts of the landscape affected by deep-seated erosion, is a contrast to existing concepts, which do not encompass the stochastic nature of weathering (Dixon and von Blanckenburg 2012; Maher and Chamberlain 2014; Riebe, Kirchner, and Finkel 2003).

Ultimately, the importance and impact of landslide weathering will be determined by the rate of the geomorphic process and the mineral composition of the substrate in which it occurs. However, it will also depend on the efficiency with which the products of mass wasting are removed from the landscape and transferred into geological basins, relative to the time needed to leach the most labile mineral phases from the mobile sediment, and to the return time of important mass wasting events in the landscape. In this light, we draw attention to the possibility that disproportionate dissolution of highly labile mineral phases such as pyrite or carbonate as a result of landslide driven weathering may reduce the strength of the feedback between erosion and atmospheric CO₂ drawdown via silicate weathering in fast eroding settings. The role of active mountain belts in the global Carbon cycle remains ambiguous.

7. Acknowledgements

We thank Meng-Long Hsieh and several of his students for sampling support and local knowledge in the Taiwan.

Assistance from Barney Ward, Claire Nichols and Kristen Cook greatly aided field campaigns. Carolin Zorn measured the anion content of the samples, and Rene Mania significantly improved landslide maps for Taiwan covering the last 20 years. Discussion with Friedhelm von Blanckenburg and A. Joshua West aided the development of the paper. R.E., N.H., and A.G conceived the study; R.E., N.H., and O.M. collected samples; O.M. generated landslide data; R.E. wrote the paper with major input from all authors. R.E. has benefited from Helmholtz Institutional funding during this project.

475 8. References

Berner, Robert A, and Zavareth Kothavala. 2001. "GEOCARB III; a Revised Model of Atmospheric CO2 over Phanerozoic Time." *American Journal of Science* 301: 182–204. doi:10.2475/ajs.294.1.56.

Bickle, Mike J., Edward T. Tipper, Albert Galy, Hazel Chapman, and Nigel Harris. 2015. "On Discrimination Between Carbonate and Silicate Inputs to Himalayan Rivers." *American Journal of Science* 315: 120–166. doi:10.2475/02.2015.02.

Blöthe, Jan Henrik, and Oliver Korup. 2013. "Millennial Lag Times in the Himalayan Sediment Routing System." Earth and Planetary Science Letters 382: 38–46. doi:10.1016/j.epsl.2013.08.044.

© Author(s) 2016. CC-BY 3.0 License.



490



- Brady, P.L. 1991. "The Effect of Silicate Weathering on Global Temperature and Atmospheric CO2." Journal of Geophysical Research 96 (91). doi:10.1029/91JB01898.
- 485 Brantley, Susan L., Molly E. Holleran, Lixin Jin, and Ekaterina Bazilevskaya. 2013. "Probing Deep Weathering in the Shale Hills Critical Zone Observatory, Pennsylvania (USA): The Hypothesis of Nested Chemical Reaction Fronts in the Subsurface." Earth Surface Processes and Landforms 38 (11): 1280–1298. doi:10.1002/esp.3415.
 - Calmels, Damien, Jérôme Gaillardet, Agnès Brenot, and Christian France-Lanord. 2007. "Sustained Sulfide Oxidation by Physical Erosion Processes in the Mackenzie River Basin: Climatic Perspectives." Geology 35 (11): 1003– 1006. doi:10.1130/G24132A.1.
 - Calmels, Damien, Albert Galy, Niels Hovius, Mike Bickle, a. Joshua West, Meng-Chiang Chen, and Hazel Chapman. 2011. "Contribution of Deep Groundwater to the Weathering Budget in a Rapidly Eroding Mountain Belt, Taiwan." Earth and Planetary Science Letters 303 (1-2) (February 15): 48–58. doi:10.1016/j.epsl.2010.12.032.
 - Central Geological Survey, Ministry of Economic Affairs. 2000. "Geologic Map of Taiwan."
- 495 Cheng, Miao-Ching, and Chen-Feng You. 2010. "Sources of Major Ions and Heavy Metals in Rainwater Associated with Typhoon Events in Southwestern Taiwan." *Journal of Geochemical Exploration* 105 (3) (June): 106–116. doi:10.1016/j.gexplo.2010.04.010.
 - Chien, Fang Ching, and Hung Chi Kuo. 2011. "On the Extreme Rainfall of Typhoon Morakot (2009)." *Journal of Geophysical Research* 116 (January): 1–22. doi:10.1029/2010JD015092.
- 500 CWB (Central Weather Bureau). 2016. Daily Precipitation Records: http://www.cwb.gov.tw/V7e/climate/dailyPrecipitation/dP.htm.
 - Dadson, Simon J., Niels Hovius, Hongey Chen, W. Brian Dade, Jiun-Chuan Lin, Mei-Ling Hsu, Ching-Weei Lin, et al. 2004. "Earthquake-Triggered Increase in Sediment Delivery from an Active Mountain Belt." *Geology* 32 (8): 733. doi:10.1130/G20639.1.
- 505 Dadson, SJ, Niels Hovius, H Chen, and WB Dade. 2003. "Links between Erosion, Runoff Variability and Seismicity in the Taiwan Orogen." *Nature* 426 (6967): 648–651.
 - Das, Anirban, Chuan-Hsiung Chung, and Chen-Feng You. 2012. "Disproportionately High Rates of Sulfide Oxidation from Mountainous River Basins of Taiwan Orogeny: Sulfur Isotope Evidence." *Geophysical Research Letters* 39 (12) (June 28) doi:10.1029/2012GL051549.
- 510 Dixon, Jean L., and Friedhelm von Blanckenburg. 2012. "Soils as Pacemakers and Limiters of Global Silicate Weathering." Comptes Rendus Geoscience 344 (11-12) (November): 597–609. doi:10.1016/j.crte.2012.10.012.
 - Emberson, Robert, Niels Hovius, Albert Galy, and Odin Marc. 2015. "Chemical Weathering in Active Mountain Belts Controlled by Stochastic Bedrock Landsliding." *Nature Geoscience*. doi:10.1038/NGEO2600.
- Fuller, Christopher W., Sean D. Willett, Niels Hovius, and Rudy Slingerland. 2003. "Erosion Rates for Taiwan

 Mountain Basins: New Determinations from Suspended Sediment Records and a Stochastic Model of Their

 Temporal Variation." *The Journal of Geology* 111 (1): 71–87. doi:10.1086/344665.
 - Gaillardet, J, B Dupré, P Louvat, and CJ Allegre. 1999. "Global Silicate Weathering and CO 2 Consumption Rates Deduced from the Chemistry of Large Rivers." Chemical Geology 159: 3–30.
- Galloway, James N, Gene E Likens, C Keene, and John M Miller. 1982. "The Composition of Precipitation in Remote Areas of the World" 87 (11): 8771–8786.
 - Galy, Albert, and Christian France-Lanord. 1999. "Weathering Processes in the Ganges–Brahmaputra Basin and the Riverine Alkalinity Budget." *Chemical Geology* 159 (1-4) (July): 31–60. doi:10.1016/S0009-2541(99)00033-9.
 - Heimsath, Arjun M., William E. Dietrich, K Nishiizumi, and R C Finkel. 1997. "The Soil Production Function and Landscape Equilibrium." *Nature* 388 (July): 21–24.

© Author(s) 2016. CC-BY 3.0 License.



530

540



- 525 Hilley, G.E., C.P. Chamberlain, S. Moon, S. Porder, and S.D. Willett. 2010. "Competition between Erosion and Reaction Kinetics in Controlling Silicate-Weathering Rates." *Earth and Planetary Science Letters* 293 (1-2) (April): 191–199. doi:10.1016/j.epsl.2010.01.008.
 - Hilton, Robert G., Jérôme Gaillardet, Damien Calmels, and Jean Louis Birck. 2014. "Geological Respiration of a Mountain Belt Revealed by the Trace Element Rhenium." Earth and Planetary Science Letters 403: 27–36. doi:10.1016/j.epsl.2014.06.021.
 - Hilton, Robert G., Albert Galy, and Niels Hovius. 2008. "Riverine Particulate Organic Carbon from an Active Mountain Belt: Importance of Landslides." *Global Biogeochemical Cycles* 22 (1) (March 15): n/a–n/a. doi:10.1029/2006GB002905.
- Hilton, Robert G., Patrick Meunier, Niels Hovius, Peter J. Bellingham, and Albert Galy. 2011. "Landslide Impact on Organic Carbon Cycling in a Temperate Montane Forest." *Earth Surface Processes and Landforms* 36 (12) (September 30): 1670–1679. doi:10.1002/esp.2191.
 - Ho, C.S. 1975. An Introduction to Geology of Taiwan. Ministry of Economic Affairs, Taipei.
 - Hovius, Niels, Patrick Meunier, Ching-Weei Lin, Hongey Chen, Yue-Gau Chen, Simon Dadson, Ming-Jame Horng, and Max Lines. 2011. "Prolonged Seismically Induced Erosion and the Mass Balance of a Large Earthquake." Earth and Planetary Science Letters 304 (3-4) (April): 347–355. doi:10.1016/j.epsl.2011.02.005.
 - Hovius, Niels, Colin P. Stark, Chu Hao-Tsu, and Lin Jiun-Chuan. 2000. "Supply and Removal of Sediment in a Landslide-Dominated Mountain Belt: Central Range, Taiwan." *The Journal of Geology* 108 (1): 73–89. doi:10.1086/314387.
- Hovius, Niels, CP Stark, and PA Allen. 1997. "Sediment Flux from a Mountain Belt Derived by Landslide Mapping." 545 *Geology* 25 (3): 231–234.
 - Hsieh, Meng-Long, and Shyh-Jeng Chyi. 2010. "Late Quaternary Mass-Wasting Records and Formation of Fan Terraces in the Chen-Yeo-Lan and Lao-Nung Catchments, Central-Southern Taiwan." *Quaternary Science Reviews* 29 (11-12) (June): 1399–1418. doi:10.1016/j.quascirev.2009.10.002.
- Kao, Shuh-ji, Chorng-shern Horng, Andrew P Roberts, and Kon-kee Liu. 2004. "Carbon Sulfur Iron Relationships in Sedimentary Rocks from Southwestern Taiwan: Influence of Geochemical Environment on Greigite and Pyrrhotite Formation." *Chemical Geology* 203: 153–168. doi:10.1016/j.chemgeo.2003.09.007.
 - Larsen, Isaac J., David R. Montgomery, and Oliver Korup. 2010. "Landslide Erosion Controlled by Hillslope Material." *Nature Geoscience* 3 (4) (February 28): 247–251. doi:10.1038/ngeo776.
- Lin, Ching Weei, Wei Shu Chang, Shou Heng Liu, Tsai Tsung Tsai, Shin Pin Lee, Yun Chung Tsang, Chjeng Lun Shieh, and Chih Ming Tseng. 2011. "Landslides Triggered by the 7 August 2009 Typhoon Morakot in Southern Taiwan." Engineering Geology 123 (1-2): 3–12. doi:10.1016/j.enggeo.2011.06.007.
 - Lin, Guan-Wei, Hongey Chen, Yi-Hui Chen, and Ming-Jame Horng. 2008. "Influence of Typhoons and Earthquakes on Rainfall-Induced Landslides and Suspended Sediments Discharge." *Engineering Geology* 97 (1-2) (March): 32–41. doi:10.1016/j.enggeo.2007.12.001.
- 560 Lyons, W. Berry. 2005. "Chemical Weathering in High-Sediment-Yielding Watersheds, New Zealand." *Journal of Geophysical Research* 110 (F1): F01008. doi:10.1029/2003JF000088.
 - Maher, K, and C P Chamberlain. 2014. "Hydrologic Regulation of Chemical Weathering and the Geologic Carbon Cycle." *Science (New York, N.Y.)* 1502 (March 13). doi:10.1126/science.1250770.
- Maher, K. 2011. "The Role of Fluid Residence Time and Topographic Scales in Determining Chemical Fluxes from Landscapes." *Earth and Planetary Science Letters* 312 (1-2) (December): 48–58. doi:10.1016/j.epsl.2011.09.040.
 - Malmstrom, Maria, Steven Banwart, Jeanette Lewenhagen, Lara Duro, and Jordi Bruno. 1996. "The Dissolution of

© Author(s) 2016. CC-BY 3.0 License.





- Biotite and Chlorite at 25 ° C in the near-Neutral pH Region." Journal of Contaminant Hydrology 21: 201–213.
- Marc, O., and N. Hovius. 2015. "Amalgamation in Landslide Maps: Effects and Automatic Detection." Natural Hazards and Earth System Sciences 15 (4): 723–733. doi:10.5194/nhess-15-723-2015.
- 570 Marc, O., N. Hovius, P. Meunier, T. Uchida, and S. Hayashi. 2015. "Transient Changes of Landslide Rates after Earthquakes." Geology 43 (10): G36961.1. doi:10.1130/G36961.1.
 - Nichol, SE, MJ Harvey, and LS Boyd. 1997. "Ten Years of Rainfall Chemistry in New Zealand." Clean Air 31 (I).
- Pankhurst, D.L., and C.A.J. Appelo. 2013. "Description of Input and Examples for PHREEQC Version 3—A Computer Program for Speciation, Batch-Reaction, One-Dimensional Transport, and Inverse Geochemical Calculations." In U.S. Geological Survey Techniques and Methods, Book 6, Chap. A43, 497.
 - Riebe, Clifford S., James W. Kirchner, and Robert C. Finkel. 2003. "Long-Term Rates of Chemical Weathering and Physical Erosion from Cosmogenic Nuclides and Geochemical Mass Balance." *Geochimica et Cosmochimica Acta* 67 (22) (November): 4411–4427. doi:10.1016/S0016-7037(03)00382-X.
- Torres, Mark a., a. Joshua West, and Gaojun Li. 2014. "Sulphide Oxidation and Carbonate Dissolution as a Source of CO2 over Geological Timescales." *Nature* 507 (7492) (March 19): 346–349. doi:10.1038/nature13030.
 - Wai, Ka Ming, Neng-Huei Lin, Sheng-Hsiang Wang, and Yukiko Dokiya. 2008. "Rainwater Chemistry at a High-Altitude Station, Mt. Lulin, Taiwan: Comparison with a Background Station, Mt. Fuji." *Journal of Geophysical Research* 113 (D6) (March 29): D06305. doi:10.1029/2006JD008248.
- West, A J, C Lin, T Lin, R G Hilton, S Liu, C Chang, K Lin, A Galy, R B Sparkes, and N Hovius. 2011. "Mobilization and Transport of Coarse Woody Debris to the Oceans Triggered by an Extreme Tropical Storm" 56 (1): 77–85. doi:10.4319/lo.2011.56.1.0077.
 - West, A.J., A Galy, and M Bickle. 2005. "Tectonic and Climatic Controls on Silicate Weathering." *Earth and Planetary Science Letters* 235 (1-2) (June 30): 211–228. doi:10.1016/j.epsl.2005.03.020. 6.
- Willett, Sean D, D Fisher, C W Fuller, E C Yeh, and C Y Lu. 2003. "Erosion Rates and Orogenic Wedge Kinematics in Taiwan Inferred from Apatite Fission Track Thermochronometry." *Geology* 31 (11): 945–948. doi:10.1130/g19702.1.

Earth Surf. Dynam. Discuss., doi:10.5194/esurf-2016-31, 2016 Manuscript under review for journal Earth Surf. Dynam. Published: 6 June 2016 © Author(s) 2016. CC-BY 3.0 License.





Figure Captions

Figure 1

Locations of sampling. Fig.1A: location of Taimali catchment and landslides sampled outside of this river in Taiwan.

Fig.1B: Taimali river, with individual streams outlined over a relief map derived from ASTER DEM. Streams are colour coded by the fraction of their area occupied by landslides (scars and deposits); individual landslides are also highlighted as they were mapped from satellite imagery, together with the alluvial fill in the channel. Locations where we sampled landslide seepage are also shown.

600 Figure 2

Cyclic- and hydrothermal-corrected dissolved Sulphate $(SO_4^{2^\circ})$ plotted against corrected Total dissolved load (TDS, above) and Calcium $(Ca^{2^+}, below)$ in seepage from landslides in the Taimali river and surrounds, as well as the Chenyoulan catchment in central Taiwan. Error bars are the total measurement uncertainty.

605 Figure 3

610

615

Normalised volume of landslides (calculated volume divided by catchment area) plotted against total dissolved load (TDS, fig A), dissolved Calcium (Ca²⁺, fig B), and dissolved Sulphate (SO₄²⁻, fig C) for streams in the Taimali river (this study) and previous numbers for catchments in the Western Southern Alps (WSA) of New Zealand (Emberson et al. 2016). Vertical error bars are total measurement uncertainty; horizontal error bars are 95% confidence intervals for volumes. Each chemical measurement has been corrected for cyclic and hydrothermal input.

Figure 4

Dissolved Sulphate (SO₄²) plotted against dissolved Silicon (SiO₂, above) and Total dissolved load (TDS, below) in streams in the Taimali river. Error bars are total measurement uncertainty. Each chemical measurement has been corrected for cyclic and hydrothermal input.

Earth Surf. Dynam. Discuss., doi:10.5194/esurf-2016-31, 2016 Manuscript under review for journal Earth Surf. Dynam. Published: 6 June 2016 © Author(s) 2016. CC-BY 3.0 License.





nal nel sot																														
Fractional Channel Fill Post Morakot																														
Fractional Channel Fill pre Morakot																														
Calcite saturation index		0.3	0.7	9.0	8.0	6.0	9.0	0.7	-0.2	0.7	9.0	9.0	0.1	1.0	1.1	0.3	0.1	1.0	1.2	6.0	N/A**	1.3	6.0	8.0	6.0	6.0	9.0	1.0	1.0	0.0
Catchment area, m ²																								3129659	496256	8467	1023265	9861469	3359874	3652240
Fractional Catchment landslide volume																								0.0001			0.0203	0.0014	0.0077	0.0414
Fractional I Catchment C landslide area																								0.0002			0.0089	0.0010	0.0030	0.0350
Example 1 Control of the control of		173825	51591	7089	66325	16264	54682	20704	63566055	206275	291661	25183	87662	608272	18525	318261	113912	44598	22298	32469	87339	284460	15310							
Landslide area, m² I (±10%) vv		83825	33676	7589	40666	14156	35180	16968	2775932 6	95319	123628	95961	50139	214670	15609	132000	61035	30188	17940	23787	20000	121000	13528							
TDS, g		11450	11131	7643	7410	13555	10665	7080	12523 2	11088	7306	9322	9397	14813	14960	8788	10267	8332	9229	12431	18738	23292	13857	2202	7094	8069	4229	0830	6243	59.88
DIC, µmol/l (±10%)		5109	3851	3595	3353	5979	5100	2582	4185	3400	2552	2583	4965	6902	4226	3674	3879	4026	2739	3810	**0	1189	1448	2699	2976	3173	2077	2901	3082	2799
SO ₄ ² ·, µmol/1 (±10%)		1453	2322	789	798	1965	1198	1366	2851	2714	1503	2450	199	1867	4080	1336	1891	749	2344	3118	10133	7827	3649	454	696	1296	235	1014	533	660
Cl., µmol/1 (±10%)		128	127	129	142	101	42	æ	18	78	88	40	27	21	26	17	16	175	34	78	24	30	27	75	101	128	100	22	66	g.
Sr ²⁺ , µmol/l C (±2%)		17	18	13	14	3	22	18	13	14	=======================================	22	9	2	6	80	6	9	19	16	83	36	56	7	Ξ	13	9	=======================================	80	ır
Si, µmol/l (±3%)		365	201	232	289	195	367	226	282	289	257	267	162	173	199	154	131	244	205	230	375	287	274	225	272	569	287	190	201	206
Na*, µmol/1 S (±6%)		571	290	469	523	559	334	317	365	415	271	381	962	452	406	807	963	541	312	305	609	983	638	381	515	513	377	326	381	318
Mg ²⁺ , μmol/l (±4%)		1016	1117	857	925	3679	185	373	179	240	41	545	1267	3476	1643	1081	1412	1187	229	153	486	1189	1448	478	029	928	237	773	562	614
i*, µmol/l (±2%)		1.92	pql	lpq	pql	5.82	lpq	ΙÞ٩	lþd	lbdl	lþd	lþd	3.42	7.52	4.38	4.80	6.19	3.45	lþd	ΙÞ٩	3.14	9.94	5.71	lþq	lþq	pql	lþq	lpq	pql	Pd
., µmol/l Li*, µmol/l (±5%)		73	43	25	42	48	43	21	168	41	46	09	34	77	29	27	33	26	39	112	120	85	42	21	25	0	19	27	20	17
Ca ²⁺ , µmol/l K ⁻ (±3%)		2716	2862	1534	1324	1019	3374	2123	4462	3946	2588	2975	1475	1666	4337	1680	1926	1373	3308	4658	6954	8344	3813	1164	1556	1801	892	1535	1357	1309
ပ		22.2	21.0	21.6	21.3	21.1	21.7	19.5	21.4	21.5	21.0	24.5	22.4	27.8	23.7	20.8	19.5	20.5	22.4	29.8	30.5	32.4	23.4	20.5	20.2	20.1	19.7	20.6	8.61	20.5
Hq T		7.63	8.23 2	8.06	8.45	8.68	7.67	8.36	7.30 2	8.26	8.29	8.26	7.49 2	8.39	7.99	7.83	7.64	8.46	8.43	7.76	8.19	7.98	7.46 2	8.42	8.40 2	8.34	8.42	8.51	8.56	8 47
Long		120.90475 7	120.94849 8	120.92747 8	120.92238 8	120.89299 8	120.87698 7	120.87584 8	120.82355 7	120.8213 8	120.8312 8	120.85339 8	120.68069 7	120.69309 8	120.66478 7	120.71692 7	7 20.71718 7	120.88542 8	120.8484 8	120.84421 7	120.846 8	7 78787 7	120.89918 7		120.94132 8	120.92323 8	120.92101 8	120.91415 8	120.91301 8	120 88979 8
Latitude I		22.52297 120	22.59528 120	22.58965 120	22.58543 120	22.57942 120	22.57541 120	22.56998 120	22.57503 120	22.58521 120	22.57556 120	22.57318 120	22.51877 120	22.53412 120	22.76694 120	22.73699 120	22.73627 120	22.44895 120	22.58739 120	22.60323 120	22.61525 12	23.61785 120	23.62402 120	22.59175 120.93216	22.59484 120	22.58802 120	22.58496 120	22.58763 120	22.58109 120	22 57508 120
Name La	ali & runds rge	TWS15-17 22.	TWS15-26 22.	FWS15-31 22.	rws15-33 22.	FWS15-38 22.	TWS15-41 22.	TWS15-42 22.	TWS15-46 22.	TWS15-47 22.	TWS15-49 22.	TWS15-51 22.	TWS15-63 22.	TWS15-65 22.	TWS15-68 22.	TWS15-72 22.	TWS15-73 22.	TWS15-86 22.	TWS15-87 22.	TWS15-90 22.	TWS15-91 22. Chenyoulan seepage	CH1307-101 23.	40	FWS15-23 22.	TWS15-25 22.	TWS15-32 22.	TWS15-34 22.	TWS15-35 22.	TWS15-36 22.	TWS15-39 22
	Taimali & Surrounds Seepage	TWS	TWS	TWS	TWS	TWS	TWS	TWS	TWS	TWS	TWS	TWS	CHI	CH1310- Taimali Streams	TWS	TWS	TWS	TWS	TWS	TWS	TWC									

© Author(s) 2016. CC-BY 3.0 License.





0.0328			0.032		0.1268	0.0332			0.0348	0.0512		
0.0			0.0		0.12	0.0			0.0	0.0		
0.0325			0.0218		0.0466	0.0214			0.0113	0		
6.0	8.0	6.0	0.5	0.7	0.7	8.0	1.1	1.0	1.2	1.1		-0.2
5461061	1211594	357320	62281990	4423928	25323473	3012380	145453	596003	5670550	4462662		
0.7246	0.0857	0.1187	0.2774	0.1005	0.2111	1.2017	0.1646	0.0637	0.3246	0.1833		
0.1665	0.0180	0.0740	0.1170	0.0690	0.0880	0.1480	0.1293	0.0170	0.1660	0.1150		
9256	5377	5327	7521	5802	7374	7657	12709	6275	12287	8388		100150
2383	2435	2145	2850	1167	1574	1990	3068	2571	2880	2711		7011
2622	617	846	1487	1778	2280	2138	3734	948	3761	1933		235
32	19	30	15	40	56	37	4	32	20	56		40124
30	6	9	7	80	13	14	21	6	22	12		∞
186	219	239	154	268	225	161	596	275	217	226		3643
322	330	247	169	301	302	296	480	348	273	336		46541
974	350	64	106	137	138	1281	346	146	172	134		28
lþq	lþq	lþq	lpq	lþq	lþq	lþq	lþq	lpq	lbdl	lpq		1191
92	30	18	30	34	78	61	78	40	129	49		862
2627	1326	1732	2703	2069	2736	1678	4642	1902	4815	2962		71
6.61	18.3	18.5	20.0	22.1	27.1	25.5	22.5	22.0	25.1	24.3		24.1
8.40	8.47	8.53	77.77	8.46	8.19	8.46	8.25	8.46	8.27	8.41		8.43
22.57427 120.88347 8.40			22.58458 120.81979 7.77	22.56602 120.84565 8.46			22.58842 120.84806	22.59241 120.84619 8.46				22.59343 120.93897 8.43 24.1
22.57427	22.56971 120.87585	22.57248 120.82725	22.58458	22.56602	22.57761 120.85395	22.57609 120.86786	22.58842	22.59241	22.62438 120.8435	22.59696 120.84148		22.59343
TWS15-40	TWS15-43	TWS15-44	TWS15-48	TWS15-50	TWS15-52	TWS15-53	TWS15-88	TWS15-89	TWS15-93	TWS15-94	Hot Spring	TWS15-22

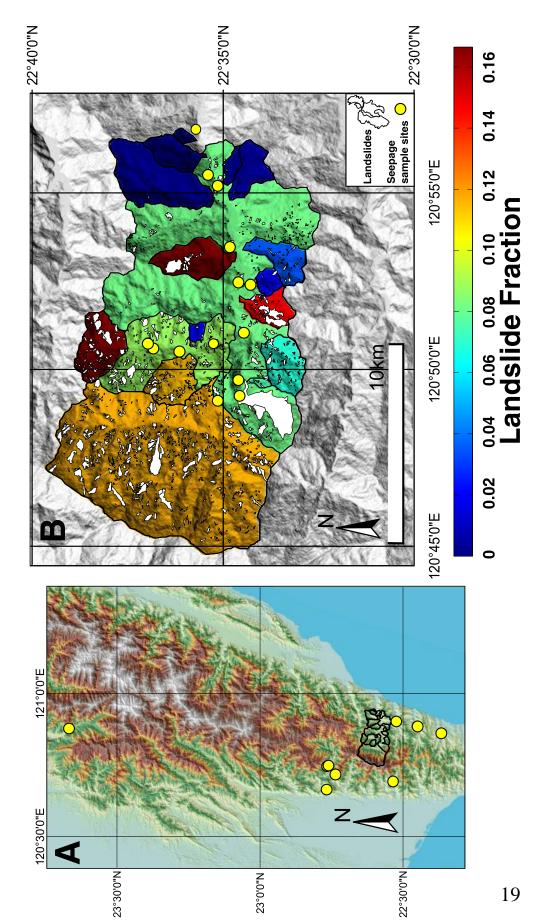
All samples are shown uncorrected for either cyclic or hydrothermal input.

** Charge balance calculations suggest no DIC, meaning a calcite saturation index is not possible to calculate.

Earth Surf. Dynam. Discuss., doi:10.5194/esurf-2016-31, 2016 Manuscript under review for journal Earth Surf. Dynam. Published: 6 June 2016 © Author(s) 2016. CC-BY 3.0 License.



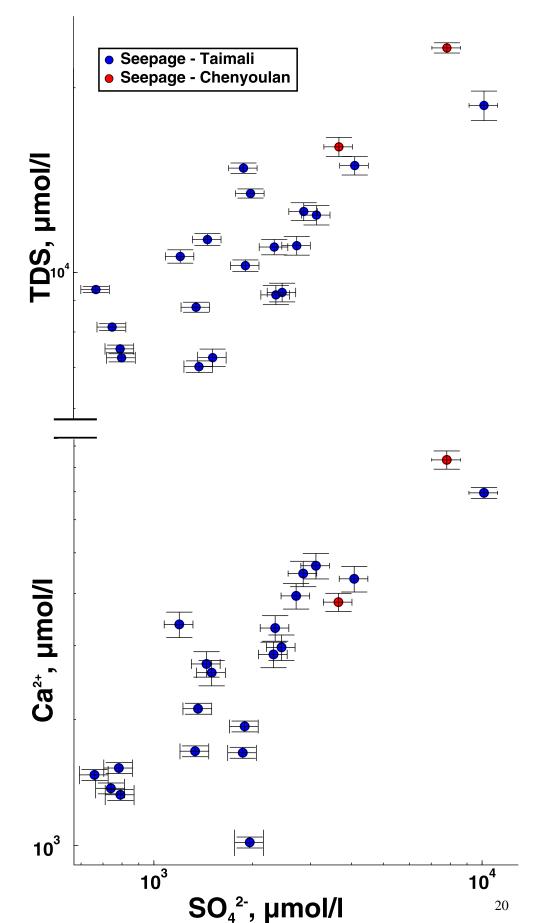




© Author(s) 2016. CC-BY 3.0 License.





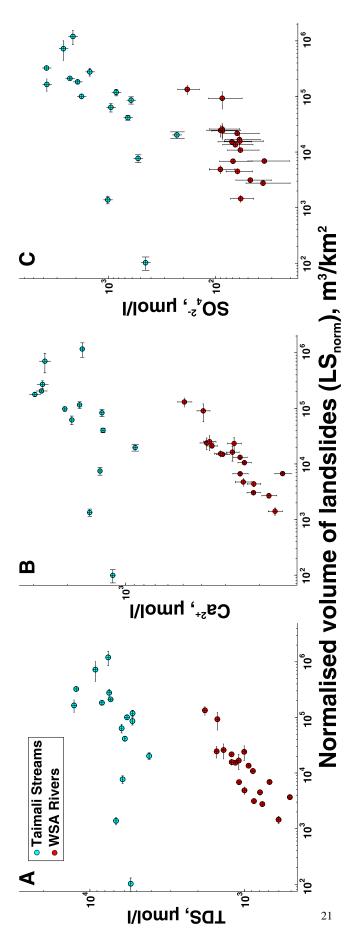


Published: 6 June 2016

© Author(s) 2016. CC-BY 3.0 License.







Earth Surf. Dynam. Discuss., doi:10.5194/esurf-2016-31, 2016 Manuscript under review for journal Earth Surf. Dynam. Published: 6 June 2016 © Author(s) 2016. CC-BY 3.0 License.





